Molecular Biology of the Cell
Vol. 20, 2909–2919, June 15, 2009

The Class V Myosin Myo2p Is Required for Fus2p Transport and Actin Polarization during the Yeast Mating Response

Jason M. Sheltzer* and Mark D. Rose

Department of Molecular Biology, Princeton University, Princeton, NJ 08544-1014

Submitted September 10, 2008; Revised March 30, 2009; Accepted April 20, 2009
Monitoring Editor: David G. Drubin

Mating yeast cells remove their cell walls and fuse their plasma membranes in a spatially restricted cell contact region. Cell wall removal is dependent on Fus2p, an amphiphysin-associated Rho-GEF homolog. As mating cells polarize, Fus2p-GFP localizes to the tip of the mating projection, where cell fusion will occur, and to cytoplasmic puncta, which show rapid movement toward the tip. Movement requires polymerized actin, whereas tip localization is dependent on both actin and a membrane protein, Fus1p. Here, we show that Fus2p-GFP movement is specifically dependent on Myo2p, a type V myosin, and not on Myo4p, another type V myosin, or Myo3p and Myo5p, type I myosins. Fus2p-GFP tip localization and actin polarization in shmoos are also dependent on Myo2p. A temperature-sensitive tropomyosin mutation and Myo2p alleles that specifically disrupt vesicle binding caused rapid loss of actin patch organization, indicating that transport is required to maintain actin polarity. Mutant shmoos lost actin polarity more rapidly than mitotic cells, suggesting that the maintenance of cell polarity in shmoos is more sensitive to perturbation. The different velocities, differential sensitivity to mutation and lack of colocalization suggest that Fus2p and Sec4p, another Myo2p cargo associated with exocytotic vesicles, reside predominantly on different cellular organelles.

INTRODUCTION

How cells create and maintain asymmetry is a fundamental problem in cell biology. In yeast cells undergoing mitotic growth, polarized secretion is directed toward the developing bud (Pruyne and Bretscher, 2000). The septin ring, which forms at the mother-daughter neck, acts as a diffusion barrier to limit the flow of asymmetrically localized proteins out of the bud (Barral *et al.*, 2000). Mating yeast must also localize proteins to specific sites on the plasma membrane, though they lack an analogous structure to prevent retrograde diffusion. How mating yeast selectively polarize certain proteins remains a largely unexplored question.

The budding yeast, *Saccharomyces cerevisiae*, has two haploid mating types, *MAT***a** and *MAT*α, which can conjugate to form a diploid cell (reviewed in Marsh and Rose, 1997). Haploid yeast cells secrete a peptide pheromone (**a-**factor or α-factor) that triggers a MAP kinase signaling cascade in cells of the opposite mating type (Bardwell, 2005). In response to pheromone, haploid cells arrest their cell cycle at G1, begin apical growth in the direction of the pheromone gradient (commonly called "shmooing"), and up-regulate the transcription of mating-specific genes (Wilkinson and Pringle, 1974; Fields *et al.*, 1988; Segall, 1993). When mating partners make contact, the intervening cell wall is degraded, and the plasma membranes fuse to form a continuous surface (Gammie *et al.*, 1998). Finally, apposing nuclei are pulled together by cytoplasmic microtubules, allowing karyogamy to occur (Meluh and Rose, 1990; Molk *et al.*, 2006). After conjugation is complete, mating-specific processes are down-regulated, and the cell is able to resume mitotic growth.

Efficient mating requires intracellular and cell surface polarization toward a mating partner (Chenevert *et al.*, 1994; Bagnat and Simons, 2002). Pheromone signaling activates the formin Bni1p, which triggers the reorganization of the actin cytoskeleton and directs new cell wall growth toward the formation of a mating projection (Evangelista *et al.*, 1997; Matheos *et al.*, 2004). Additionally, proteins required for cell wall degradation localize to the tip of the mating projection, where cell fusion will occur. Fus1p and Fus2p have been identified as key mediators of cell fusion: both proteins localize to the shmoo tip, and crosses between *fus1* or *fus2* pairs result in profound mating defects (Trueheart *et al.*, 1987; Elion *et al.*, 1995). Fus1p is an O-glycosylated membrane-spanning protein that regulates fusion pore formation (Nolan *et al.*, 2006), whereas Fus2p is a cytoplasmic protein that contains a putative guanine-nucleotide exchange factor (GEF) domain and may be involved in transduction of the fusion signal (Paterson *et al.*, 2008). Fus2p acts in conjunction with Rvs161p, a BAR domain–containing, amphiphysin-like protein that has various roles in endocytosis and vesicular trafficking (Crouzet *et al.*, 1991; Sivadon *et al.*, 1995; Brizzio *et al.*, 1998; Friesen *et al.*, 2006; Paterson *et al.*, 2008). Because BAR domain proteins typically form dimers that interact with the curved surfaces of membranes (Peter *et al.*, 2004), Fus2p-Rvs161p heterodimers may localize to the surface of vesicles that have been observed to cluster at the junction between mating cells (Gammie *et al.*, 1998; Paterson *et al.*, 2008).

In a recent study, Paterson *et al.* (2008) tagged Fus2p with green fluorescent protein (GFP) to observe Fus2p dynamics

This article was published online ahead of print in *MBC in Press* (http://www.molbiolcell.org/cgi/doi/10.1091/mbc.E08–09–0923) on April 29, 2009.

* Present address: Department of Biology, Massachusetts Institute of Technology, Cambridge, MA 02139.

Address correspondence to: Mark D. Rose (mdrose@princeton.edu).

Supplemental Material can be found at:
http://www.molbiolcell.org/content/suppl/2009/04/27/E08-09-0923.DC1.html

in vivo. In shmoos, Fus2p-GFP was found to localize primarily to the tip of the mating projection. Surprisingly, Fus2p-GFP also appeared as cytoplasmic puncta that were observed moving rapidly toward the shmoo tip. Puncta movement was dependent on polymerized actin, whereas Fus2p-GFP's localization to the shmoo tip was dependent on both actin and Fus1p, which may also function as a cortical anchor.

In *S. cerevisiae*, actin-dependent motility occurs via one or more members of the myosin family of molecular motors, or via Arp2/3-mediated actin polymerization (Brown, 1997; Bretscher, 2003). The classical type II myosin, Myo1p, is required for cytokinesis. The type I myosins, Myo3p and Myo5p, function during the internalization step of endocytosis, and the type V myosins, Myo2p and Myo4p, transport various cargoes along actin cables. Myo2p is implicated in vesicular and organelle transport, whereas Myo4p is known to transport mRNA and elements of the cortical endoplasmic reticulum (ER). The actin-nucleating ability of Arp2/3 may drive the movement of mitochondria and endosomes (Boldogh *et al.*, 2001; Chang *et al.*, 2003), although this function remains controversial (Itoh *et al.*, 2002; Altmann *et al.*, 2008).

In this study, we sought to identify the protein(s) responsible for Fus2p's actin-dependent movement. We find that Fus2p is transported by Myo2p along actin cables to the shmoo tip, where it becomes anchored to the plasma membrane by Fus1p. Fus2p transport was distinct from the transport of Sec4p, suggesting that the majority of these proteins reside on distinct cellular structures. Surprisingly, actin organization was highly dependent on both Myo2p and tropomyosin in shmoos but not in mitotic cells, suggesting that the maintenance of cytoskeletal polarity differs between these growth regimes.

MATERIALS AND METHODS

General Yeast Techniques

Yeast manipulations and general techniques were performed as previously described (Rose *et al.*, 1990). Temperature-sensitive strains were grown at 23°C; all other strains were grown at 30°C. For induction with mating pheromone, cultures were grown to early log phase and then treated with synthetic alpha-factor (Department of Molecular Biology Syn/Seq Facility, Princeton University) to a final concentration of 10 μg/ml. Temperature-sensitive strains were incubated in pheromone for 120 min at 23°C; all other strains were incubated in pheromone for 90 min at 30°C.

Strain and Plasmid Construction

Yeast strains and plasmids used in this study are listed in Tables 1 and 2. *FUS1* disruptions were performed using one-step gene replacement. The Fus2p-mCherryFP construct (pMR5821) was created by in vivo recombination (Oldenburg *et al.*, 1997). Three fragments were generated by PCR to form the construct. A PCR fragment containing homology to the vector along with 500 base pairs of the 5′ untranslated region (UTR) plus the first 360 base pairs of *FUS2* was amplified with primers JP21 (vector sequence is in uppercase letters, *FUS2* sequence is in lowercase letters: TAGGGCGAATTGGGTACCGGGCCCCCCCTCGAGGTCGACGGTATCGATgtcccacctgcttggtgg) and RC Fus2-mChFP (CCTCCTCGCCCTTGCTCACCATGGGAATCTGAGGGCTCAAATTCAGTCTCACGAC) using genomic DNA as a template. A second PCR fragment containing the mCherry fluorescent protein coding sequence with flanking *FUS2* homology was amplified from pMR5598 using primers Fus2-mChFP (GTCGTGAGACTGAATTTGAGCCCTCAGATTCCCATGGTGAGCAAGGGCGAGGAGG) and mChFP-Fus2106 (ATAAAATTTGCATCCCTCGTGAGGAGAATTCTTGTACAGCTCGTCCATGCCG). A third fragment containing the C-terminal portion of *FUS2* and homology to the vector was amplified using primers RC mChFP-Fus2106 (CGGCATGGACGAGCTGTACAAGAATTCTCCTCACGAGGGATGCAAATTTTAT) and JP22 (vector sequence is in uppercase letters, *FUS2* sequence is in lowercase letters: GCTGGAGCTCCACCGCGGTGGCGGCCGCTCTAGAACTAGTGGATCCCCctgctccagcgcagtagt) with genomic DNA as the template. The three PCR products were transformed along with the pRS415 vector cut with BamHI into a *fus2*Δ strain. Plasmid DNA was extracted from the transformants and the *FUS2-mCherryFP* fusion construct was confirmed by restriction digestion. The functionality was verified by complementation of the *fus2* mating defect and by localization of Fus2p-mCherryFP in response to pheromone.

Live Cell Microscopy

To visualize GFP fluorescence, early log phase cells were incubated with pheromone then placed on an agar pad containing the appropriate selective media supplemented with 10 μg/ml alpha factor. Cells were visualized using a DeltaVision deconvolution microscope (Applied Precision, Issaquah, WA), based on a Nikon TE200 (Melville, NY), using a 100× objective, a 50 W Hg lamp, and a Cool Snap ER CCD camera (Roper Scientific, Trenton, NJ). For short time courses, images were acquired every 0.36 or 0.46 s using 0.2-s exposures and 2 × 2 binning. For Z sections, 24 images were acquired at a spacing of 0.2 μm, using 0.4-s exposures, 2 × 2 binning, and a 93% neutral density filter. GFP fluorescence was visualized using a FITC filter set (Chroma, Brattleboro, VT).

Temperature-shift assays were conducted using the Delta T4 Culture Dish System (Bioptechs, Butler, PA), and 0.17-mm culture dishes (Bioptechs) were coated with 20 μl of concanavalin-A (0.1 mg/ml in 20 mM NaOAc, pH 5.8) for 5 min and then washed three times with phosphate-buffered saline (PBS). Early log phase cells that had been pretreated with pheromone were then transferred onto the dish and allowed to bind for 5 min. After binding, excess medium was removed, and fresh medium supplemented with 10 μg/ml alpha factor was added. Dishes were placed on a Delta T4 stage Adapter (Bioptechs) and visualized as described above.

Actin Staining

To visualize actin, cells were fixed for 10 min in 4% formaldehyde and then washed twice with PBS. Subsequently, cells were resuspended in 50 μl of PBS and treated with 25 μl of Texas red-phalloidin (Molecular Probes, Eugene, OR) for 1 h in the dark. Cells were washed three times with PBS and then placed on agarose pads for microscopy. Texas red-phalloidin staining was visualized using a rhodamine filter set.

Immunofluorescence Microscopy

Indirect immunofluorescence of Sec4p was performed as previously described (Walch-Solimena *et al.*, 1997). Cells were treated with pheromone for 1.5 h at 23°C and shifted to 37°C for varying times before fixation. mAb C123 against Sec4p, a generous gift of P. Novick (UC San Diego, CA), was used undiluted. To detect the anti-Sec4p, Alexafluor 64–conjugated goat anti-mouse secondary antibody (Molecular Probes) was used at 1:500, and cells were visualized using a Cy5 filter set.

Image Analysis

Images were deconvolved and collapsed for analysis using the SoftWorx Imaging software (Applied Precision). Velocity measurements were made on deconvolved images using SoftWorx. For publication purposes, image brightness and contrast were linearly increased, and where needed, pixel density was resampled using a bicubic algorithm in Photoshop CS3 (Adobe, San Jose, CA).

RESULTS

Myo2p Is Required for the Localization of Fus2p

Paterson *et al.* (2008) previously demonstrated that Fus2p is transported via an actin-dependent process to the tip of the mating projection, where it is anchored to the plasma membrane by Fus1p. To identify the protein(s) responsible for Fus2p movement, we examined the distribution of Fus2p in strains containing deletions or conditional mutations in the various yeast myosins. The type II myosin encoded by *MYO1* was excluded from our initial survey of the yeast myosin family, because it has no known function in yeast outside of cytokinesis and its expression is down-regulated in the presence of pheromone (Brown, 1997; Roberts *et al.*, 2000). Additionally, because *MYO3* and *MYO5* are partially redundant, we utilized a *myo3*Δ *myo5*Δ strain in which growth was rescued by a plasmid carrying a temperature-sensitive allele of *MYO5* (*myo5-1*; Geli and Riezman, 1996).

Fus2p-GFP localized to the shmoo tip normally in both *myo4*Δ *FUS1* and *myo4*Δ *fus1*Δ strains (Figure 1). Consistent with previous observations, Fus2p-GFP was visible as a dense spot at the tip of the mating projection in pheromone-treated *FUS1* cells, but assumed a broader distribution in *fus1*Δ strains. Fus2p localization was also unaffected in pheromone-treated *myo3*Δ *myo5*Δ [*myo5-1*] *FUS1* and

Table 1. Yeast strains used in this study

Strain	Genotype	Plasmid	Source
ABY535	*MAT***a** *ade2-101 his3Δ200 leu2-3,112 lys2-801 ura3-52 myo2-66::HIS3*		A. Bretscher, Cornell U.
ABY551	*MAT***a**/*MATα ade2-101/ade2-101 his3Δ200/his3Δ200 leu2-3,112/leu2-3,112 lys2-801/lys2-801 ura3-52/ura3-52 MYO2::HIS3/MYO2::HIS3*		A. Bretscher, Cornell U.
ABY553	*MAT***a**/*MATα ade2-101/ade2-101 his3Δ200/his3Δ200 leu2-3,112/leu2-3,112 lys2-801/lys2-801 ura3-52/ura3-52 myo2-16::HIS3/myo2-16::HIS3*		A. Bretscher, Cornell U.
ABY2180	*MAT***a** *ade2-101 his3Δ200 leu2-3,112 lys2-801 ura3-52*		A. Bretscher, Cornell U.
ABY2404	*MAT***a** *ade2 can1 his3 leu2 trp1 ura3 myo2-0IQ::HIS3*		A. Bretscher, Cornell U.
ABY2406	*MAT***a** *ade2 can1 his3 leu2 trp1 ura3 myo2-2IQ::HIS3*		A. Bretscher, Cornell U.
ABY2408	*MAT***a** *ade2 can1 his3 leu2 trp1 ura3 myo2-4IQ::HIS3*		A. Bretscher, Cornell U.
ABY2410	*MAT***a** *ade2 can1 his3 leu2 trp1 ura3 myo2-6IQ::HIS3*		A. Bretscher, Cornell U.
LWY5475	*MAT***a** *ura3-52 leu2-3,112 his3-Δ200 trp1-Δ901 lys2-801 suc2-Δ9 myo2Δ::TRP1, Ycp50_MYO2*		L. Weisman, U. of Michigan
LWY5875	*MAT***a** *ura3-52 leu2-3,112 his3-Δ200 trp1-Δ901 lys2-801 suc2-Δ9 myo2Δ::TRP1, pRS413_myo2-D1297N*		L. Weisman, U. of Michigan
LWY5877	*MAT***a** *ura3-52 leu2-3,112 his3-Δ200 trp1-Δ901 lys2-801 suc2-Δ9 myo2Δ::TRP1, pRS413_myo2-L1301P*		L. Weisman, U. of Michigan
LWY5897	*MAT***a** *ura3-52 leu2-3,112 his3-Δ200 trp1-Δ901 lys2-801 suc2-Δ9 myo2Δ::TRP1, pRS413_MYO2*		L. Weisman, U. of Michigan
LWY5898	*MAT***a** *ura3-52 leu2-3,112 his3-Δ200 trp1-Δ901 lys2-801 suc2-Δ9 myo2Δ::TRP1, pRS413_myo2-G1248D*		L. Weisman, U. of Michigan
LWY7488	*MATα ura3-52 leu2-3,112 his3-Δ200 trp1-Δ901 lys2-801 suc2-Δ9 myo2Δ::TRP1, pRS413_myo2-Y1415E*		L. Weisman, U. of Michigan
LWY7522	*MATα ura3-52 leu2-3,112 his3-Δ200 trp1-Δ901 lys2-801 suc2-Δ9 myo2Δ::TRP1, pRS413_myo2-K1444A*		L. Weisman, U. of Michigan
NY130	*MAT***a** *ura3-52 sec2-41*		P. Novick, UCSD
RH3376	*MAT***a** *his3 leu2 trp1 bar1*		H. Riezman, U. of Basel
RH3383	*MAT***a** *his3 leu2 trp1 bar1 myo3Δ::HIS3 myo5Δ::TRP1* [*myo5-1 URA3*]		H. Riezman, U. of Basel
MY10037	*MAT***a** *his3Δ1 leu2Δ0 ura3Δ0 met15Δ0*	pMR5482	This study
MY10039	*MAT***a** *his3Δ1 leu2Δ0 ura3Δ0 met15Δ0 myo4Δ::KanMX*	pMR5482	This study
MY10155	*MAT***a** *ade2-101 his3Δ200 leu2-3,112 lys2-801 ura3-52 MYO2::HIS3*		This study
MY10157	*MAT***a** *ade2-101 his3Δ200 leu2-3,112 lys2-801 ura3-52 myo2-16::HIS3*		This study
MY10203	*MAT***a** *ade2-101 his3Δ200 leu2-3,112 lys2-801 ura3-52*	pMR5482	This study
MY10204	*MAT***a** *ade2-101 his3Δ200 leu2-3,112 lys2-801 ura3-52 myo2-66::HIS3*	pMR5482	This study
MY10366	*MAT***a** *his3 leu2 trp1 bar1 fus1Δ::KanMX*	pMR5643	This study
MY10385	*MAT***a** *his3 leu2 trp1 bar1 myo3Δ::HIS3 myo5Δ::TRP1 fus1Δ::KanMX* [*myo5-1 URA3*]	pMR5643	This study
MY10408	*MAT***a** *his3Δ1 leu2Δ0 ura3Δ0 met15Δ0 fus1Δ::NatMX*	pMR5482	This study
MY10409	*MAT***a** *his3Δ1 leu2Δ0 ura3Δ0 met15Δ0 myo4Δ::KanMX fus1Δ::NatMX*	pMR5482	This study
MY10412	*MAT***a** *ade2-101 his3Δ200 leu2-3,112 lys2-801 ura3-52 myo2-16::HIS3 fus1Δ::KanMX*	pMR5482	This study
MY10413	*MAT***a** *ade2-101 his3Δ200 leu2-3,112 lys2-801 ura3-52 myo2-66::HIS3 fus1Δ::KanMX*	pMR5482	This study
MY10418	*MAT***a** *ade2 can1 his3 leu2 trp1 ura3 myo2-2IQ::HIS3*	pMR5482	This study
MY10419	*MAT***a** *ade2 can1 his3 leu2 trp1 ura3 myo2-4IQ::HIS3*	pMR5482	This study
MY10420	*MAT***a** *ade2 can1 his3 leu2 trp1 ura3 myo2-6IQ::HIS3*	pMR5482	This study
MY10433	*MAT***a** *ade2 can1 his3 leu2 trp1 ura3 myo2-2IQ::HIS3 fus1Δ::KanMX*	pMR5482	This study
MY10434	*MAT***a** *ade2 can1 his3 leu2 trp1 ura3 myo2-4IQ::HIS3 fus1Δ::KanMX*	pMR5482	This study
MY10437	*MAT***a** *ade2 can1 his3 leu2 trp1 ura3 myo2-0IQ::HIS3*	pMR5482	This study
MY10443	*MAT***a** *ade2 can1 his3 leu2 trp1 ura3 myo2-0IQ::HIS3 fus1Δ::KanMX*	pMR5482	This study
MY10444	*MAT***a** *ade2 can1 his3 leu2 trp1 ura3 myo2-6IQ::HIS3 fus1Δ::KanMX*	pMR5482	This study
MY10495	*MAT***a** *ade2 can1 his3 leu2 trp1 ura3 myo2-6IQ::HIS3 fus1Δ::KanMX*	pRC651	This study
MY10502	*MAT***a** *ade2-101 his3Δ200 leu2-3,112 lys2-801 ura3-52 myo2-16::HIS3*	pMR5482	This study
MY10512	*MAT***a** *ade2-101 his3Δ200 leu2-3,112 lys2-801 ura3-52 fus1Δ::NatMX*	pMR5482	This study
MY10525	*MAT***a** *his3 leu2 trp1 bar1*	pMR5643	This study
MY10529	*MAT***a** *his3 leu2 trp1 bar1 myo3Δ::HIS3 myo5Δ::TRP1* [*myo5–1 URA3*]	pMR5643	This study
MY10530	*MAT***a** *ade2 can1 his3 leu2 trp1 ura3 myo2-6IQ::HIS3 fus1Δ::KanMX*	pMR5821 pMR5877	This study
MY10717	*MAT***a** *ura3-52 leu2-3,112 his3-Δ200 trp1-Δ901 lys2-801 suc2-Δ9 myo2Δ::TRP1, pRS413_MYO2*	pMR5482	This study
MY10718	*MAT***a** *ura3-52 leu2-3,112 his3-Δ200 trp1-Δ901 lys2-801 suc2-Δ9 myo2Δ::TRP1, pRS413_myo2-G1248D*	pMR5482	This study
MY10719	*MAT***a** *ura3-52 leu2-3,112 his3-Δ200 trp1-Δ901 lys2-801 suc2-Δ9 myo2Δ::TRP1, pRS413_myo2-G1297N*	pMR5482	This study
MY10746	*MAT***a** *ade2-101 his3Δ200 leu2-3,112 lys2-801 ura3-52 myo2-16::HIS3*	pRC651	This study
MY10748	*MATα ura3-52 leu2-3,112 his3-Δ200 trp1-Δ901 lys2-801 suc2-Δ9 myo2Δ::TRP1, pRS413_myo2-Y1415E*	pMR5643	This study
MY10749	*MATα ura3-52 leu2-3,112 his3-Δ200 trp1-Δ901 lys2-801 suc2-Δ9 myo2Δ::TRP1, pRS413_myo2-K1444A*	pMR5643	This study

Table 2. Plasmids used in this study

Plasmid	Genotype/Description	Source
pRC651	*SEC4::GFP LEU2 CEN3 ARS1 AMP^R*	A. Bretscher, Cornell University
pMR5482	*FUS2::GFP URA3 CEN3 ARS1 AMP^R*	Paterson *et al.* (2008)
pMR5598	*mCherryFP KanMX6 AMP^R*	S. Clark, Princeton University
pMR5643	*FUS2::GFP LEU2 CEN3 ARS1 AMP^R*	C. A. Ydenberg, Princeton University
pMR5821	*FUS2::mCherryFP LEU2 CEN3 ARS1 AMP^R*	This study
pMR5877	*SEC4::GFP leu2::URA3 CEN3 ARS1 AMP^R*	This study

*myo3*Δ *myo5*Δ [*myo5-1*] *fus1*Δ cells that were incubated at the restrictive temperature for 30 min (Figure 1B). In wild-type and *myo4*Δ and *myo3/5*Δ strains, cytoplasmic puncta were observed moving in a linear manner toward the tip of the mating projection (see Supplementary Videos 1–3), providing a further indication that transport of Fus2p is independent of these three proteins.

We next assayed the localization of Fus2p in two strains containing conditional mutations in the *MYO2* gene. The *myo2-16* and *myo2-66* strains harbor temperature-sensitive mutations in the actin-binding head domain and cargo-binding tail domain, respectively, of *MYO2* (Lillie and Brown, 1994; Schott *et al.*, 1999). Fus2p was partially mislocalized at both the permissive and restrictive temperature in *FUS1* cells harboring the *myo2* mutations, with *myo2-66* showing a more severe defect (Figure 2A). At 24 and 36°C, more Fus2p puncta were visible in the cytoplasm of the *myo2-66 FUS1* and *myo2-16 FUS1* cells, relative to the wild type, with the number of puncta increasing at the higher temperature. However, for both mutants, Fus2p-GFP remained enriched at the shmoo tip in *FUS1* cells (Figure 2A). Significantly, directed movement of Fus2p puncta was not observed in the *myo2* mutants that had been incubated at the restrictive temperature for 5 min or longer (see Supplementary Video 4).

Deletion of *FUS1* in strains that contained the mutant *myo2* alleles fully abolished Fus2p localization to the shmoo tip (Figure 2B). Within 5 min of shifting *myo2-16 fus1*Δ and *myo2-66 fus1*Δ cells to the restrictive temperature, the polarized localization of Fus2p to the shmoo tip was lost in >95% of cells, and Fus2p assumed a random distribution throughout the cytoplasm. We concluded that Myo2p is required to maintain the polarized localization of Fus2p.

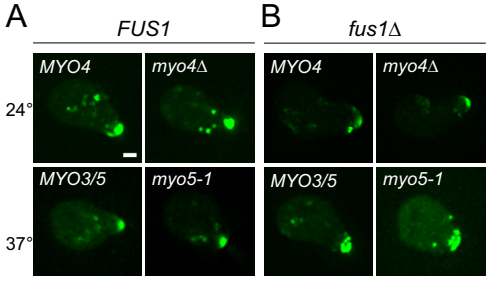

Figure 1. Fus2p localizes as normal in *myo4*Δ and *myo3/5*Δ [*myo5-1*] cells. (A) Fus2p-GFP localization in *MYO4* (MY10037), *myo4*Δ (MY10039), *MYO3/5* (MY10525), and *myo3*Δ *myo5*Δ [*myo5-1*] (MY10529). (B) Fus2p-GFP localization in *MYO4 fus1*Δ (MY10408), *myo4*Δ *fus1*Δ (MY10409), *MYO3/5 fus1*Δ (MY10366), and *myo3*Δ *myo5*Δ [*myo5-1*] *fus1*Δ (MY10385). Strains MY10525, MY10529, MY10366, and MY10385 (bottom row) were grown at 24°C, incubated at 37°C for 20 min before imaging, and microscopy was performed at 37°C. At least 25 shmoos of each genotype were examined, and representative images are displayed. Scale bar, 1 μm.

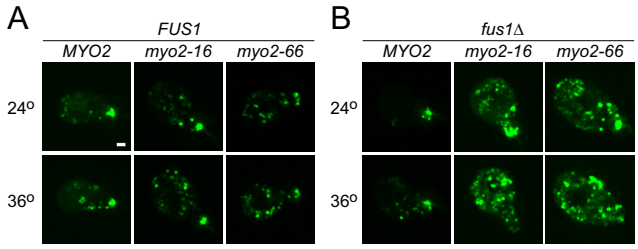

Figure 2. Myo2p is required for Fus2p localization. (A) Fus2p-GFP localization in *MYO2* (MY10203), *myo2-16* (MY10502), and *myo2-66* (MY10204). (B) Fus2p-GFP localization in *MYO2 fus1*Δ (MY10512), *myo2-16 fus1*Δ (MY10412), and *myo2-66 fus1*Δ (MY10413). Cells were first visualized at 24°C, then the temperature was raised to 36°C for 5 min and the same cells were imaged again. At least 30 shmoos of each genotype were examined, and representative images are displayed. Scale bar, 1 μm.

Myo2p Is Required for Cytoskeletal Polarity in Shmoos

Myo2p has several functions in cell growth and polarization, and mutations in the *MYO2* gene have been reported to cause pleiotropic defects in a variety of cellular processes (Govindan *et al.*, 1995; Schott *et al.*, 1999). In particular, the *myo2-66* allele has been demonstrated to abolish the polarization of the actin cytoskeleton in mitotic cells grown at the restrictive temperature (Johnston *et al.*, 1991). Because polarized actin is required for Fus2p transport, the loss of Fus2p localization observed in the *myo2* mutants may have been due to defects in cytoskeletal polarity. Therefore, we examined the actin cytoskeleton in pheromone-treated cells that contained mutations in *MYO2*.

To observe the distribution of actin, cells were fixed and stained with Texas red–conjugated phalloidin. In wild-type shmoos, both filamentous actin cables and cortical actin patches polarized toward the tip of the mating projection (Figure 3A). In *myo2-66* shmoos formed at the permissive temperature, actin organization was indistinguishable from wild-type. However, when *myo2-66* cells were fixed and examined after 5 min at 36°C, actin patches were dispersed across the cell cortex, and cables were randomly oriented throughout the cell (Figure 3A). Thus, the mislocalization of Fus2p at the restrictive temperature in *myo2-66* could have been the result of an indirect effect of the myosin mutation.

To distinguish Myo2p's role in actin organization from its role in vesicular transport, various temperature-sensitive alleles of *MYO2* with mutations in the cargo-binding tail domain have been generated (Schott *et al.*, 1999). Although *myo2-66* disrupts many, if not all, of Myo2p's functions, the *myo2-16* mutation was identified as a temperature-sensitive allele of *MYO2* that specifically blocked vesicular transport without perturbing cytoskeletal organization after short incubations at the restrictive temperature. We first confirmed the observations of Schott *et al.* (1999) in mitotic cells. The *myo2-16* cells grown at the permissive temperature contained actin cables and patches polarized toward the developing bud (Figure 3B). Incubation at 35°C for 5 min had no noticeable effect on actin organization in mitotic cells, and both cables and patches remained aligned in the direction of

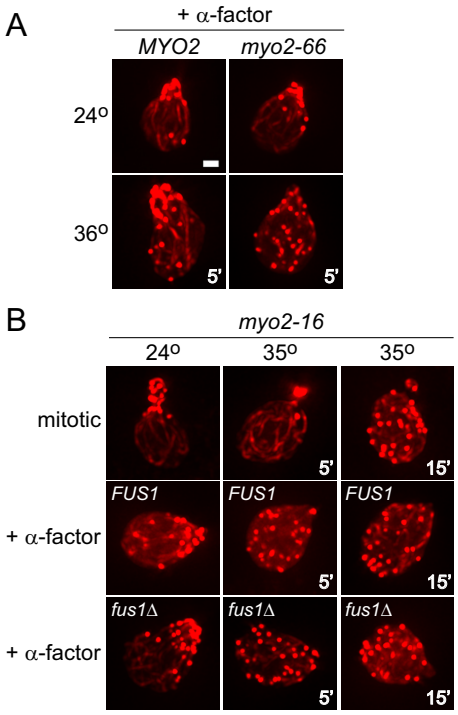

Figure 3. Myo2p is required for cytoskeletal polarity in shmoos. (A) Texas red-phalloidin staining of *MYO2 fus1*Δ (MY10512) and *myo2-66 fus1*Δ (MY10413). Pheromone-treated cells were either fixed and stained at 24°C (top row) or incubated at 36°C for 5 min (bottom row) before fixation. (B) Texas red-phalloidin staining of *myo2-16* (MY10157) and *myo2-16 fus1*Δ (MY10412). Mitotically growing cells (top row) and pheromone-treated cells (bottom rows) were either fixed and stained at 24°C or incubated at 35°C for 5 or 15 min before fixation. At least 20 shmoos of each genotype were examined under each experimental condition, and representative images are displayed. Scale bar, 1 μm.

cell growth. Only after 15 min at the restrictive temperature did actin polarization become visibly aberrant, with actin patches randomly distributed over the entire cell cortex. Surprisingly, we found that the cytoskeleton responded differently to the inactivation of Myo2p in pheromone-treated cells. Actin polarized normally at the permissive temperature in *myo2-16* shmoos. However, *myo2-16* shmoos that had been shifted to the restrictive temperature for 5 min failed to maintain actin polarization and instead showed cytoskeletal disorganization similar to *myo2-66*. The depolarization of actin in *myo2-16* shmoos occurred in both *FUS1* and *fus1*Δ strains. We concluded that the maintenance of actin polarization in pheromone-treated cells is exquisitely sensitive to Myo2p function, and therefore we could not yet rule out the possibility that the defect in Fus2p localization in *myo2-16* is an indirect effect of a general defect in cytoskeletal polarity.

Accordingly, we next sought to find an intermediate temperature between 24 and 36°C at which Fus2p might become delocalized while the cytoskeleton remained polarized. Fus2p localization was examined in *myo2-16 fus1*Δ and *myo2-66 fus1*Δ cells as we gradually increased the temperature in increments of 3°C (Figure 4A). For both mutants, Fus2p became completely delocalized, and all directed movement of Fus2p puncta ceased at 33°C and above. However, Texas red–conjugated phalloidin staining of actin in parallel cultures revealed that cytoskeletal organization also was aberrant at 33°C (Figure 4B). From these results, we concluded that Fus2p localization is tightly associated with

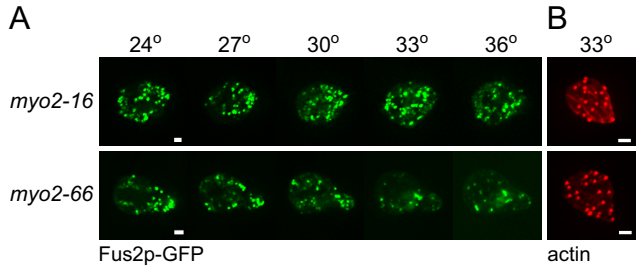

Figure 4. Fus2p and the actin cytoskeleton are delocalized at a semirestrictive temperature in *myo2-16* and *myo2-66*. (A) Fus2p-GFP localization in *myo2-16 fus1*Δ (MY10412) and *myo2-66 fus1*Δ (MY10413). Shmoos were first examined at 24°C, and then the temperature was raised by 3°C. After a 10-min incubation at the new temperature, the same cells were examined again, and this process was repeated until the temperature reached 36°C. (B) Texas red-phalloidin staining of MY10412 and MY10413. After identifying 33°C as the temperature at which Fus2p delocalizes, fresh cells were incubated at 33°C for 10 min, then fixed and stained for actin. Scale bars, 1 μm.

Myo2p function, but we were unable to separate Myo2p's role in cytoskeletal polarization from its potential role in Fus2p transport.

Tropomyosin Is Required to Maintain Actin Patch Polarity in Shmoos

We next sought to determine whether the defect in actin organization observed in *myo2-16* shmoos was a unique consequence of the defect in Myo2p function or whether mutations in other cytoskeletal proteins would show a similar lack of actin stability in pheromone-treated cells. We therefore examined the actin cytoskeleton in a *tpm1-2 tpm2*Δ strain. In mitotic cells incubated at 34.5°C, this strain rapidly loses actin cables, whereas actin patches remain polarized in the growing bud (Pruyne *et al.*, 1998).

Actin polarized as normal at the permissive temperature in *tpm1-2 tpm2*Δ cells (Figure 5). In mitotic cells, after 5 min at the restrictive temperature actin cables were no longer visible, although the polarized distribution of actin patches remained unaffected. Only after 15 min at 34.5°C did the actin patches become dispersed throughout the mother and daughter. In contrast, pheromone-treated *tpm1-2 tpm2*Δ cells lost both actin cables and the polarized distribution of actin patches after a 5-min incubation at 34.5°C (Figure 5). Similar

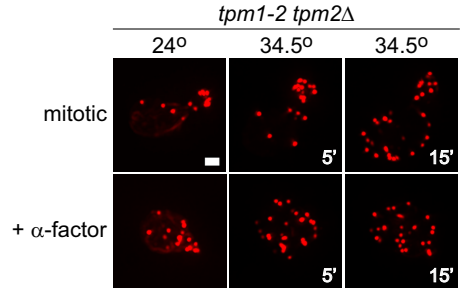

Figure 5. Tropomyosin is required to maintain actin patch polarity in shmoos. Texas red-phalloidin staining of *tpm1-2 tpm2*Δ (ABY944). Mitotically growing or pheromone-treated cells were either fixed and stained at 24°C or incubated at 35°C for 5 or 15 min before fixation. At least 20 shmoos were examined under each experimental condition, and representative images are displayed. Scale bars, 1 μm.

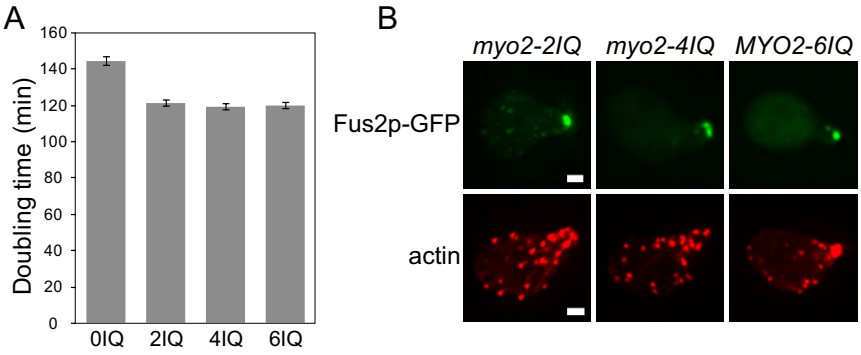

Figure 6. Myo2p mutants with 2 or 4 IQ repeats grow and polarize normally. (A) Doubling time during exponential growth of *myo2-0IQ* (ABY2404), *myo2-2IQ* (ABY2406), *myo2-4IQ* (ABY2408), and *MYO2-6IQ* (ABY2410). (B) Fus2p-GFP localization and Texas red-phalloidin staining of *myo2-2IQ* (MY10418), *myo2-4IQ* (MY10419), and *MYO2-6IQ* (MY10420).

results were obtained after 15 min at the restrictive temperature. Our findings with *myo2-16* and *tpm1-2 tpm2*Δ cells suggest that during pheromone-induced polarization, the actin cytoskeleton is more sensitive to perturbation than during mitotic growth.

The Speed of Fus2p Puncta Varies with the Length of the Myo2p Lever Arm Domain

Because we were unable to separate the delocalization of Fus2p from the effects of actin depolarization using the *myo2-16* and *myo2-66* alleles, we adopted a different strategy, based on the physical properties of the class V myosin protein, to determine whether or not Myo2p actively transports Fus2p along actin cables. According to the swinging lever arm model of myosin transport, myosin delivers cargo by walking hand-overhand along actin cables, and the length of the neck region determines the step size that myosin can take (Purcell *et al.*, 2002). Correspondingly, myosin alleles that have artificially shortened neck domains move along actin filaments at a slower rate in vitro than the wild-type protein (Uyeda *et al.*, 1996). In *S. cerevisiae*, Schott *et al.* (2002) utilized a GFP-tagged Sec4p construct to demonstrate in vivo that the velocity of secretory vesicles transported by Myo2p varied with the number of IQ repeats present in the Myo2p neck domain. We therefore sought to determine whether the velocity of Fus2p-GFP puncta showed a similar dependence on the length of the Myo2p lever arm.

We first examined the pheromone response, growth rate, and cytoskeletal organization in cells in which the wild-type allele of *MYO2* (*MYO2-6IQ*) had been replaced by alleles harboring zero, two, or four repeats of the IQ neck domain. The *myo2-0IQ* strain grew ~20% more slowly than the isogenic wild-type strain, and after induction with pheromone, *myo2-0IQ* cells showed an abnormally high amount of autofluorescence, precluding further analysis of Fus2p-GFP localization. However, the *myo2-2IQ* and *myo2-4IQ* strains grew at the same rate as the *MYO2-6IQ* wild-type strain, responded normally to pheromone, and localized Fus2p-GFP to the shmoo tip properly (Figure 6). Importantly, we also found that actin cable and actin patch polarization were normal in pheromone-treated *myo2-2IQ* and *myo2-4IQ* cells. We concluded that any change in Fus2p velocity observed in these strains would be the result of an intrinsic change in Myo2p's motility and not an indirect effect of Myo2p's role in other cellular processes.

To calculate the velocity of the Fus2p puncta, we examined shmoos by time-lapse microscopy, acquiring images about three times per second. Puncta showing linear movement over several frames were identified, and the distance that each traveled between consecutive frames was used to generate a series of velocity measurements. The largest distance that individual puncta moved between any two successive frames was used to define the "maximum" velocity at which the puncta traveled. Presumably intervals of slower velocity observed in vivo reflect interactions of the cargo with the surrounding cytoplasmic matrix that impede movement. We chose to compare the average maximum velocity between strains with varying numbers of IQ repeats, rather than the overall average velocity, because previous work (Schott *et al.*, 2002) suggested that the maximum velocity in vivo is most directly related to the number of IQ repeats.

The average maximum speed of Fus2p-GFP puncta in the wild-type (6IQ) strain was 1.94 ± 0.08 μm/s (SEM, n = 75 puncta). Strikingly, the average maximum speed of Fus2p puncta was significantly reduced in *myo2-4IQ* and *myo2-2IQ* cells (Figure 7 and Supplementary Video 5). The average maximum velocity of Fus2p-GFP puncta in the *myo2-4IQ* mutant was 1.42 ± 0.05 μm/s (SEM, n = 75, $p \leq 0.0001$ relative to wild type). The velocity was further reduced in the *myo2-2IQ* mutant to only 1.22 ± 0.05 μm/s (SEM, n = 75, $p \leq 0.0001$ relative to wild type). Additionally, the highest maximum speed observed for a single punctum was 3.84 μm/s in wild type, 2.68 μm/s in the *myo2-4IQ* mutant, and 2.46 μm/s in the *myo2-2IQ* mutant. We also measured the maximum velocities of Fus2p puncta in *myo4*Δ cells and

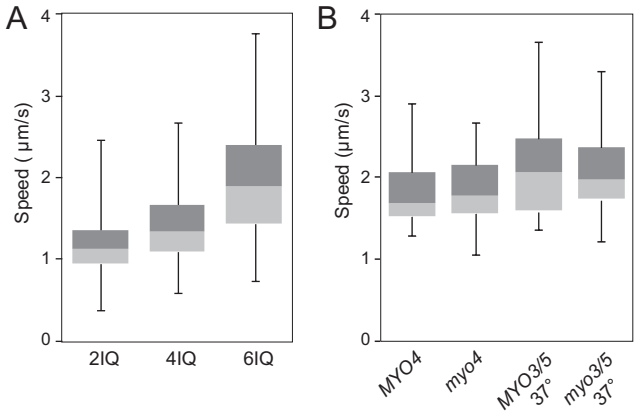

Figure 7. The speed of Fus2p puncta varies with the length of the Myo2p lever arm domain. Box plot of maximum puncta speed in (A) *myo2-2IQ fus1*Δ (MY10433), *myo2-4IQ fus1*Δ (MY10434), and *MYO2-6IQ fus1*Δ (MY10444) and (B) *MYO4 fus1*Δ (MY10408), *myo4*Δ *fus1*Δ (MY10409), *MYO3/5 fus1*Δ (MY10366), and *myo3*Δ *myo5*Δ [m*yo5-1*] *fus1*Δ (MY10385). The boxes represent the middle quartiles of data collected, and the whiskers represent the range. Microscopy of strains MY10366 and MY10368 was performed at 37°C, all other strains were imaged at 24–26°C.

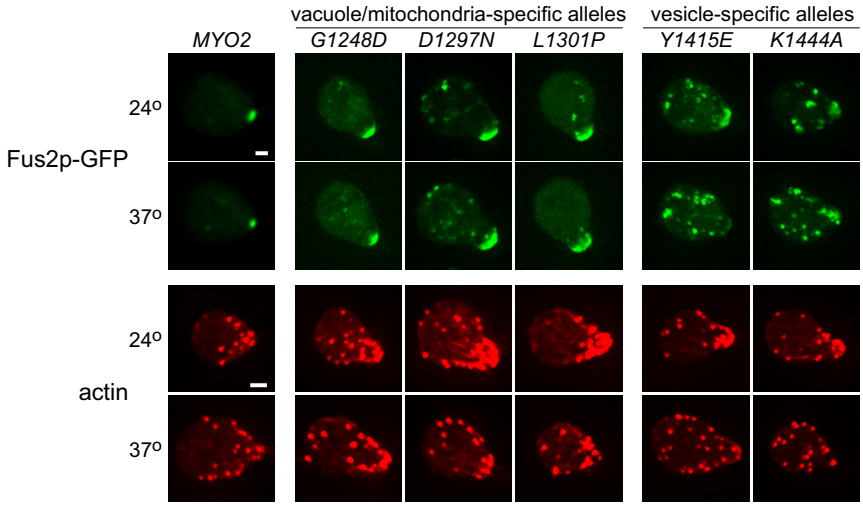

Figure 8. MYO2 alleles which block vesicular transport also perturb actin organization and Fus2p localization. Fus2p-GFP localization and Texas red-phalloidin staining of *MYO2* (MY10717), *myo2-G1248D* (MY10718), *myo2-D1297N* (MY10719), *myo2-L1301P* (MY10720), *myo2-Y1415E* (MY10748), and *myo2-K1444A* (MY10749). For Fus2p-GFP visualization, cells were first imaged at 24°C, then the temperature was raised to 37°C for 5 min and the same cells were imaged again. For Texas red-phalloidin staining, pheromone-treated cells were either fixed and stained at 24°C or incubated at 37°C for 5 min before fixation.

*myo3/5*Δ [*myo5-1*] cells incubated at 37°C, along with their isogenic wild-type strains. Fus2p-GFP puncta velocities in these mutant strains did not differ significantly from the velocities observed in the wild-type strains (Figure 7B). Because the speed of Fus2p puncta varied with the length of the Myo2p lever arm, but was not affected by the inactivation of Myo4p and Myo3/5p, we conclude that Myo2p is responsible for the transport of Fus2p along actin cables.

Myo2p's Vesicle-binding Function Is Required for Actin Polarity and Fus2p Localization

Because Rvs161p is associated with membranes (Friesen *et al.*, 2006) and Fus2p fractionates with vesicular or cytoskeletal structures (Elion *et al.*, 1995), it was previously proposed that the Fus2p-GFP puncta represent Fus2p-Rvs161p heterodimers localized to secretory vesicles (Paterson *et al.*, 2008). We used temperature-sensitive alleles of Myo2p that block the transport of specific organelles to gather evidence for this hypothesis.

The globular tail of Myo2p has two functional subdomains that interact with different cargoes: subdomain I is the site of vacuolar and mitochondrial attachment, whereas subdomain II is the site of secretory vesicle attachment (Catlett *et al.*, 2000; Pashkova *et al.*, 2005; Altmann *et al.*, 2008). Point mutations within these domains have been identified that specifically block Myo2p's transport of different cargoes. To clarify Myo2p's role in mating cell polarization, we examined Fus2p-GFP localization and the actin cytoskeleton in strains harboring mutations in either subdomain I or II; *myo2-G1248D*, *myo2-D1297N*, and *myo2-L1301P* contain mutations in subdomain I, whereas *myo2-Y1415E* and *myo2-K1444A* contain mutations in subdomain II. At 37°C, *myo2-G1248D* and *myo2-D1297N* block transport of vacuoles (Catlett and Weisman, 1998; Catlett *et al.*, 2000), *myo2-L1301P* blocks transport of vacuoles and mitochondria (Catlett *et al.*, 2000; Altmann *et al.*, 2008), and *myo2-Y1415E* and *myo2-K1444A* block transport of secretory vesicles (Pashkova *et al.*, 2005). We found that Fus2p-GFP localization and actin polarization were specifically affected by point mutations that interfere with vesicular transport (Figure 8). At the restrictive temperature, actin polarization was aberrant in *myo2-K1444A* and *myo2-Y1415E*, but not in *myo2-G1248D*, *myo2-D1297N*, and *myo2-L1301P*. Similarly, in *myo2-K1444A* and *myo2-Y1415E*, but not in any other mutant, a significant fraction of Fus2p-GFP failed to localize to the shmoo tip at the restrictive temperature, and numerous Fus2p-GFP puncta were visible in the cytoplasm. These results suggest that a vesicular or vesicle-associated cargo is responsible for promoting cytoskeletal polarity. Additionally, though we cannot rule out the possibility that the delocalization of Fus2p was an indirect effect of the myosin mutation, these results are consistent with a model for cellular fusion in which Fus2p localizes to the surface of vesicles.

Fus2p Transport Is Distinct from the Transport of Sec4p-marked Secretory Vesicles

During polarized growth, secretory vesicles that carry the Rab GTPase Sec4p are transported to the plasma membrane by Myo2p (Schott *et al.*, 2002). Despite evidence suggesting that Fus2p may associate with vesicles (Elion *et al.*, 1995; Paterson *et al.*, 2008; Figure 7), we were surprised to find that the average maximum velocity of Fus2p-GFP puncta in pheromone-treated cells (1.94 μm/s) was markedly slower than the reported average velocity of Sec4p-GFP puncta in mitotic cells (~3 μm/s; Schott *et al.*, 2002). Because both Fus2p and Sec4p are putative membrane-associated cargo transported by Myo2p, we determined whether the different velocities reflect different rates of transport between mating and mitotic cells or localization of Fus2p and Sec4p to different populations of vesicles or organelles. First, we measured the velocity of Sec4p-GFP puncta in pheromone-treated cells (Figure 9A, Supplementary Video 6). Strikingly, the Sec4p-GFP puncta traveled at an average maximum velocity of 2.67 ± 0.13 μm/s (SEM, n = 50) in shmoos, significantly faster than the observed speed of 1.94 μm/s for Fus2p puncta ($p < 0.0001$). Furthermore, we found that the velocity of Sec4p-GFP puncta did not vary significantly between mating and mitotic cells (2.67 ± 0.13 vs. 2.96 ± 0.15 μm/s, n = 46). Second, if Sec4p and Fus2p are associated with the same cellular structures at the cortex, then Fus1p should be sufficient to retain the polarized localization of a portion of Sec4p-GFP in pheromone-treated cells after Myo2p has been inactivated. Although a fraction of Fus2p-GFP was retained at the shmoo tip at the restrictive temperature in *myo2-16 FUS1* cells, Sec4p-GFP dispersed entirely under the same conditions (Figure 9B).

At the plasma membrane, Sec4p is activated by the guanine-nucleotide exchange factor Sec2p, and Sec2p has been found to be required for Sec4p localization (Walch-Solimena *et al.*, 1997). We therefore examined the distribution of Fus2p

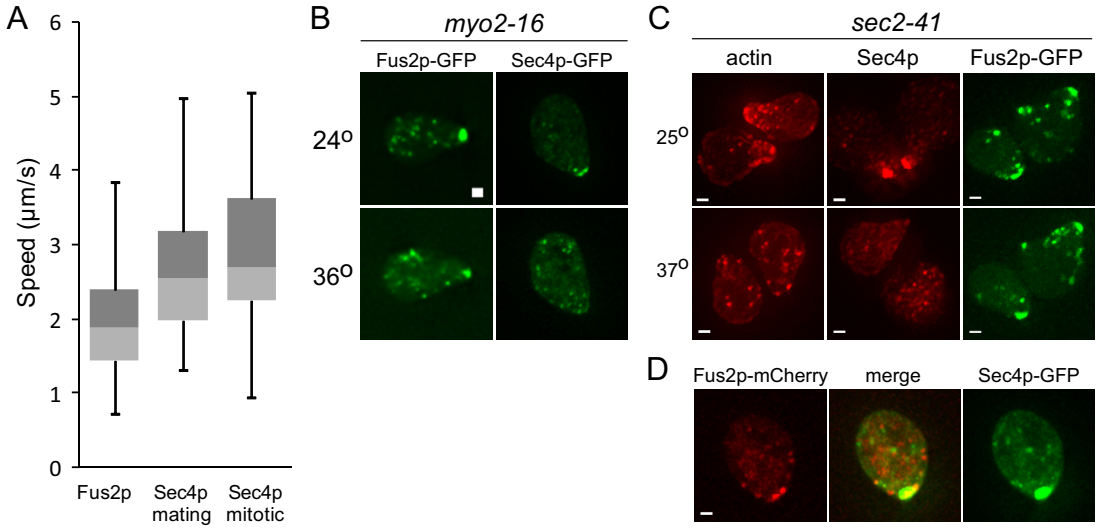

Figure 9. Fus2p and Sec4p are predominantly associated with different Myo2p cargoes. (A) Box plot of maximum Sec4p-GFP puncta speed and Fus2p puncta speed in MY10495 and MY10444, respectively. (B) Fus2p-GFP and Sec4p-GFP localization in *myo2-16* (MY10502 and MY10746, respectively). (C) Fus2p-GFP localization, Texas red-phalloidin staining, and indirect immunofluorescence of Sec4p in *sec2-41* (NY130). Pheromone-treated cells were incubated for 10 min at 37°C before visualization or fixation. For Fus2p-GFP the same cells are shown before and after the temperature shift. (D) Colocalization of Fus2p-mCherryFP and Sec4p-GFP in MY10530.

and Sec4p in a strain harboring a temperature-sensitive allele of *SEC2*. Because *SEC4* on a CEN plasmid partially suppresses *sec2* mutations (Salminen and Novick, 1987), we opted to observe Sec4p in *sec2-41* by immunofluorescence microscopy. After *sec2-41* shmoos were shifted to the restrictive temperature, actin cortical patches remained partially polarized in 60% of cells after 5 min, but only in 17% after 10 min (Figure 9C). In the isogenic wild-type control strain, actin remained polarized in 87 and 71% of cells after 5 and 10 min, respectively, at 37°C. After the temperature shift, Sec4p rapidly dispersed; showing localization to the shmoo tip in only 47% of cells after 5 min and 17% after 10 min. Unexpectedly, localization of Sec4p at the shmoo tip was also decreased in the isogenic wild-type strain to similar extents (48 and 15% after 5 and 10 min, respectively). Regardless, in both the *sec2-41* and isogenic wild-type strain, Fus2p-GFP remained localized to the shmoo tip after shift to the nonpermissive temperature; >85% of cells retained Fus2p-GFP after >10 min at the restrictive temperature. In addition to retention at the shmoo-tip, Fus2p-GFP in the cytoplasm remained punctate and showed directed movement at the nonpermissive temperature, suggesting that movement on actin cables was not impaired. Taken together these results indicate that the localization of Fus2p is independent of the localization of Sec4p.

Finally, to allow colocalization with Sec4p-GFP, we tagged *FUS2* internally with the fluorescent epitope mCherryFP (Shaner *et al.*, 2004). When Fus2p-mCherryFP and Sec4p-GFP were coexpressed in pheromone-treated cells that had been fixed to arrest puncta movement, both proteins were detectable at the shmoo tip, but did not appear to colocalize elsewhere at the cortex or in the cytoplasm (Figure 9D). In 25 shmoos examined, Fus2p-mCherryFP and Sec4p-GFP were visible throughout the cell as discrete, nonoverlapping dots. We conclude that Sec4p and Fus2p localize predominantly to different cargoes transported by Myo2p during mating. However, we cannot rule out the possibility that a minor fraction of Sec4p remains associated with Fus2p-marked vesicles or organelles, which was not detected by our assays.

DISCUSSION

To identify the protein(s) responsible for Fus2p transport, yeast strains harboring mutations in the various myosins were examined. Among the yeast myosin genes, only mutations in the class V myosin, Myo2p, compromised Fus2p localization and transport. The strongest evidence in support of a role for Myo2p in Fus2p transport was the observation that the average maximum speed of Fus2p puncta was significantly reduced in mutants in which the length of the Myo2p neck domain was decreased. We conclude that Myo2p transports Fus2p along actin cables to the shmoo tip during yeast mating.

During polarization in response to pheromone, the actin cytoskeleton becomes oriented toward the shmoo tip. Consequently, new cell surface growth and secretion occurs primarily at the shmoo tip, and proteins associated with the secretory pathway and/or actin transport will necessarily become initially concentrated in the mating projection. Retention of cell fusion proteins at the shmoo tip is required to prevent mislocalized and/or ectopic activation of the fusion machinery. Retention at the shmoo tip may arise from multiple mechanisms, including slow diffusion coupled with endocytic recycling (e.g., Snc1p; Valdez-Taubas and Pelham, 2003), stable association with distinct lipid microdomains (e.g., Fus1p; Bagnat and Simons, 2002; Jin *et al.*, 2008), and protein–protein interactions. In the case of Fus2p, retention is dependent on both Fus1p and one or more components of the actin cytoskeleton. We cannot yet determine whether Myo2p plays a direct role in Fus2p retention, because all mutations that cause loss of Fus2p-GFP localization also cause loss of actin polarization.

An unexpected result of the work described in this study is the differential stability of actin polarization in mitotic cells and in shmoos. We found that mitotic *myo2-16* and *tpm1-2* cells retained normal cytoskeletal polarization after short incubations at the restrictive temperature, whereas actin polarity was very rapidly lost in pheromone-treated *myo2-16* and *tpm1-2* cells under identical conditions. Furthermore, actin polarization in shmoos was specifically im-

paired in the *myo2* mutants with defects in vesicle binding and not mutants with defects in vacuole and/or mitochondria binding. These findings, along with other recent results, suggest a positive feedback loop between actin-dependent transport and polarization of the cytoskeleton (Pruyne *et al.*, 1998; Wedlich-Soldner *et al.*, 2003; Aronov and Gerst, 2004; Pruyne *et al.*, 2004). According to one model, cell polarity in yeast is established by the Rho-GTPase Cdc42p, which activates actin assembly via the formin family of proteins (Park and Bi, 2007). Localized deposition of Cdc42p at intrinsic spatial markers (i.e., the bud site in mitotic yeast) is supplemented by the actin-dependent delivery of Cdc42p, creating a feedback loop for robust cell polarization. Cdc42p is a putative vesicle-associated cargo of Myo2p (Wedlich-Soldner *et al.*, 2003), and mutations that break this feedback loop (i.e., by blocking steps in the late secretory pathway) cause aberrant cytoskeletal polarity (Aronov and Gerst, 2004). Thus, the loss of polarization that we observed in myosin and tropomyosin mutants may be due to the mislocalization of Cdc42p.

The different kinetics for the loss of actin polarity between mitotic cells and shmoos suggest that mitotic cells have a more robust system to maintain cell polarization. One major difference between the two cell types is the structure of the bud neck. Mitotic yeast cells have a ring of septins, a specialized structure formed by the copolymerization of four GTPases, at the cortex at the mother-bud neck (Longtine *et al.*, 1996). The septin ring is required for the maintenance of components of the yeast polarisome in the bud, and cells with temperature-sensitive mutations in the septins lose actin polarity at the restrictive temperature (Barral *et al.*, 2000). It has been proposed that the septin ring forms a passive diffusion barrier which prevents the flow of polarizing factors out of the daughter cell. Thus, when the cytoskeleton is perturbed by the inactivation of Tpm1p or Myo2p in mitotic cells, polarity may be partially maintained by the septin ring. In mating cells, septins form a more diffuse band of fibers around the neck of the shmoo oriented toward the shmoo tip (Longtine *et al.*, 1998; L. Silverstein and M. Rose, unpublished observations). Although the role of the septins during conjugation is not clear, they do not appear to function as a diffusion barrier for cortical membrane proteins between the tip of the shmoo and the cell body (Proszynski *et al.*, 2006). Therefore, in shmoos, once the actomyosin transport system is disrupted, there would be no barrier to prevent the rapid diffusion of polarity proteins (presumably including Cdc42p) throughout the cell.

Based on its localization to cellular regions containing high concentrations of vesicles and the membrane affinity of its binding partner, Rvs161p, it has been proposed that Fus2p is associated with vesicles that carry hydrolytic enzymes required for cell wall degradation (Paterson *et al.*, 2008). At the zone of cell fusion, Fus2p may trigger the release of the vesicular cargo via interaction between its Rho-GEF domain and a Rho-GTPase. The finding that Myo2p, a transporter of membrane-bound organelles, also transports Fus2p puncta supports the hypothesis that Fus2p is associated with membrane-bound organelles.

In *S. cerevisiae*, vesicle trafficking is controlled by a family of 11 Rab GTPases that function in vesicle budding, vesicle tethering, and the fusion of vesicles with their target membranes (Lazar *et al.*, 1997; Grosshans *et al.*, 2006). Each Rab GTPase is believed to act at a defined step in the trafficking pathway, and Sec4p has been identified as the Rab GTPase specifically required for the fusion of exocytotic secretory vesicles with the plasma membrane (Walch-Solimena *et al.*, 1997; Novick and Guo, 2002). We found that Fus2p puncta and Sec4p puncta were transported at significantly different speeds, and Fus2p-mCherryFP did not appear to colocalize with Sec4p-GFP in cytoplasmic puncta. We have also found that Fus2p is able to stay associated with the shmoo tip under conditions in which Sec4p does not, including in *myo2-16* and *sec2-41* shmoos. At this time, we cannot rule out the possibility that an interaction occurs between Sec4p and Fus2p-marked cargo specifically at the shmoo tip or that a minor fraction of Sec4p associates with Fus2p-marked cargo during transport. However, taken together, our observations suggest that Fus2p and Sec4p localize predominantly to different populations of vesicles or organelles that are transported by Myo2p.

The existence of multiple classes of vesicles has been demonstrated in mitotic yeast cells (Harsay and Bretscher, 1995); however, trafficking in shmoos remains relatively unexplored. Interestingly, two groups have reported that the average size of vesicles found at the shmoo tip is significantly smaller than the average size of vesicles found in budding cells (Baba *et al.*, 1989; Breton *et al.*, 2001). Thus it is possible that vesicle formation and trafficking occur via somewhat different mechanisms in pheromone-treated cells and in mitotic cells. In support of this hypothesis, Fus1p, which is not expressed in mitotic cells, appears to play a role in the clustering or anchoring of vesicles to the shmoo tip during mating (Gammie *et al.*, 1998).

Our findings therefore suggest that during the pheromone response, Myo2p transports at least two distinct classes of membrane-bound cargo. The first class constitutes the canonical, Sec4p-associated vesicles bound for the plasma membrane. These vesicles presumably carry cell wall components that are required for the formation of a mating projection and are tethered to the plasma membrane by the exocyst complex (Whyte and Munro, 2002). The second class of cargo is marked by Fus2p and is specifically required for cell fusion. This cargo may include hydrolytic enzymes necessary for cell wall degradation and would be anchored to the cortex by a complex including Fus1p, rather than the exocyst. Fusion of this cargo to the plasma membrane would be triggered by a signal generated by prezygote formation and may require the activity of the Fus2p GEF domain. The existence of distinct classes of vesicles or organelles would allow cells to fulfill the two opposing requirements for efficient mating: first, cells must grow and add cell wall in the direction of the pheromone gradient and second, cells must be able to specifically degrade their cell wall during zygote formation.

ACKNOWLEDGMENTS

We thank Casey Ydenberg for help and advice in the early stages of this project and Jason Rogers and Alison Gammie for the construction of the *FUS2-mCherryFP* plasmid. We thank Anthony Bretscher (Cornell University), Lois Weisman (University of Michigan), Peter Novick, and Howard Riezman (University of Geneva) for providing numerous helpful strains and plasmids. This work was supported by National Institutes of Health Grant GM37739.

REFERENCES

Altmann, K., Frank, M., Neumann, D., Jakobs, S., and Westermann, B. (2008). The class V myosin motor protein, Myo2, plays a major role in mitochondrial motility in *Saccharomyces cerevisiae*. J. Cell Biol. *181*, 119–130.

Aronov, S., and Gerst, J. E. (2004). Involvement of the late secretory pathway in actin regulation and mRNA transport in yeast. J. Biol. Chem. *279*, 36962–36971.

Baba, M., Baba, N., Ohsumi, Y., Kanaya, K., and Osumi, M. (1989). Three-dimensional analysis of morphogenesis induced by mating pheromone alpha factor in *Saccharomyces cerevisiae*. J. Cell Sci. *94*, 207–216.

Bagnat, M., and Simons, K. (2002). Cell surface polarization during yeast mating. Proc. Natl. Acad. Sci. USA *99*, 14183–14188.

Bardwell, L. (2005). A walk-through of the yeast mating pheromone response pathway. Peptides *26*, 339–350.

Barral, Y., Mermall, V., Mooseker, M. S., and Snyder, M. (2000). Compartmentalization of the cell cortex by septins is required for maintenance of cell polarity in yeast. Mol. Cell *5*, 841–851.

Boldogh, I. R., Yang, H.-C., Nowakowski, W. D., Karmon, S. L., Hays, L. G., Yates, J. R., and Pon, L. A. (2001). Arp2/3 complex and actin dynamics are required for actin-based mitochondrial motility in yeast. Proc. Natl. Acad. Sci. USA *98*, 3162–3167.

Breton, A. M., Schaeffer, J., and Aigle, M. (2001). The yeast Rvs161 and Rvs167 proteins are involved in secretory vesicles targeting the plasma membrane and in cell integrity. Yeast *18*, 1053–1068.

Bretscher, A. (2003). Polarized growth and organelle segregation in yeast: the tracks, motors, and receptors. J. Cell Biol. *160*, 811–816.

Brizzio, V., Gammie, A. E., and Rose, M. D. (1998). Rvs161p interacts with Fus2p to promote cell fusion in *Saccharomyces cerevisiae*. J. Cell Biol. *141*, 567–584.

Brown, S. S. (1997). Myosins in yeast. Curr. Opin. Cell Biol. *9*, 44–48.

Catlett, N. L., Duex, J. E., Tang, F., and Weisman, L. S. (2000). Two distinct regions in a yeast myosin-V tail domain are required for the movement of different cargoes. J. Cell Biol. *150*, 513–526.

Catlett, N. L., and Weisman, L. S. (1998). The terminal tail region of a yeast myosin-V mediates its attachment to vacuole membranes and sites of polarized growth. Proc. Natl. Acad. Sci. USA *95*, 14799–14804.

Chang, F. S., Stefan, C. J., and Blumer, K. J. (2003). A WASp homolog powers actin polymerization-dependent motility of endosomes in vivo. Curr. Biol. *13*, 455–463.

Chenevert, J., Valtz, N., and Herskowitz, I. (1994). Identification of genes required for normal pheromone-induced cell polarization in *Saccharomyces cerevisiae*. Genetics *136*, 1287–1297.

Crouzet, M., Urdaci, M., Dulau, L., and Aigle, M. (1991). Yeast mutant affected for viability upon nutrient starvation: characterization and cloning of the *RVS161* gene. Yeast *7*, 727–743.

Elion, E. A., Trueheart, J., and Fink, G. R. (1995). Fus2 localizes near the site of cell fusion and is required for both cell fusion and nuclear alignment during zygote formation. J. Cell Biol. *130*, 1283–1296.

Evangelista, M., Blundell, K., Longtine, M. S., Chow, C. J., Adames, N., Pringle, J. R., Peter, M., and Boone, C. (1997). bni1p, a yeast formin linking Cdc42p and the actin cytoskeleton during polarized morphogenesis. Science *276*, 118–122.

Fields, S., Chaleff, D. T., and Sprague, G. F. (1988). Yeast *STE7*, *STE11*, and *STE12* genes are required for expression of cell-type-specific genes. Mol. Cell. Biol. *8*, 551–556.

Friesen, H., Humphries, C., Ho, Y., Schub, O., Colwill, K., and Andrews, B. (2006). Characterization of the yeast amphiphysins Rvs161p and Rvs167p reveals roles for the Rvs heterodimer in vivo. Mol. Biol. Cell *17*, 1306–1321.

Gammie, A. E., Brizzio, V., and Rose, M. D. (1998). Distinct morphological phenotypes of cell fusion mutants. Mol. Biol. Cell *9*, 1395–1410.

Geli, M. I., and Riezman, H. (1996). Role of type I myosins in receptor-mediated endocytosis in yeast. Science *272*, 533–535.

Govindan, B., Bowser, R., and Novick, P. (1995). The role of Myo2, a yeast class V myosin, in vesicular transport. J. Cell Biol. *128*, 1055–1068.

Grosshans, B. L., Ortiz, D., and Novick, P. (2006). Rabs and their effectors: achieving specificity in membrane traffic. Proc. Natl. Acad. Sci. USA *103*, 11821–11827.

Harsay, E., and Bretscher, A. (1995). Parallel secretory pathways to the cell surface in yeast. J. Cell Biol. *131*, 297–310.

Itoh, T., Watabe, A., Toh-E, A., and Matsui, Y. (2002). Complex formation with Ypt11p, a rab-type small GTPase, is essential to facilitate the function of Myo2p, a class V myosin, in mitochondrial distribution in *Saccharomyces cerevisiae*. Mol. Cell. Biol. *22*, 7744–7757.

Jin, H., McCaffery, J. M., and Grote, E. (2008). Ergosterol promotes pheromone signaling and plasma membrane fusion in mating yeast. J. Cell Biol. *180*, 813–826.

Johnston, G. C., Prendergast, J. A., and Singer, R. A. (1991). The *Saccharomyces cerevisiae MYO2* gene encodes an essential myosin for vectorial transport of vesicles. J. Cell Biol. *113*, 539–551.

Lazar, T., Gotte, M., and Gallwitz, D. (1997). Vesicular transport: how many Ypt/Rab-GTPases make a eukaryotic cell? Trends Biochem. Sci. *22*, 468–472.

Lillie, S. H., and Brown, S. S. (1994). Immunofluorescence localization of the unconventional myosin, Myo2p, and the putative kinesin-related protein, Smy1p, to the same regions of polarized growth in *Saccharomyces cerevisiae*. J. Cell Biol. *125*, 825–842.

Longtine, M. S., DeMarini, D. J., Valencik, M. L., Al-Awar, O. S., Fares, H., De Virgilio, C., and Pringle, J. R. (1996). The septins: roles in cytokinesis and other processes. Curr. Opin. Cell Biol. *8*, 106–119.

Longtine, M. S., Fares, H., and Pringle, J. R. (1998). Role of the yeast Gin4p protein kinase in septin assembly and the relationship between septin assembly and septin function. J. Cell Biol. *143*, 719–736.

Marsh, L., and Rose, M.D. (1997). The pathway of cell and nuclear fusion during mating in *S. cerevisiae*. In: The Molecular and Cellular Biology of the Yeast *Saccharomyces*: Cell Cycle and Cell Biology, ed. J. R. Broach, J. R. Pringle, and E. W. Jones, Cold Spring Harbor, NY: Cold Spring Harbor Laboratory Press, 827–888.

Matheos, D., Metodiev, M., Muller, E., Stone, D., and Rose, M. D. (2004). Pheromone-induced polarization is dependent on the Fus3p MAPK acting through the formin Bni1p. J. Cell Biol. *165*, 99–109.

Meluh, P.B., and Rose, M.D. (1990). KAR3, a kinesin-related gene required for yeast nuclear fusion. Cell *60*, 1029–1041.

Molk, J. N., Salmon, E. D., and Bloom, K. (2006). Nuclear congression is driven by cytoplasmic microtubule plus end interactions in *S. cerevisiae*. J. Cell Biol. *172*, 27–39.

Nolan, S., Cowan, A. E., Koppel, D. E., Jin, H., and Grote, E. (2006). FUS1 Regulates the opening and expansion of fusion pores between mating yeast. Mol. Biol. Cell *17*, 2439–2450.

Novick, P., and Guo, W. (2002). Ras family therapy: Rab, Rho and Ral talk to the exocyst. Trends Cell Biol. *12*, 247–249.

Oldenburg, K. R., Vo, K. T., Michaelis, S., and Paddon, C. (1997). Recombination-mediated PCR-directed plasmid construction in vivo in yeast. Nucleic Acids Res. *25*, 451–452.

Park, H. O., and Bi, E. (2007). Central roles of small GTPases in the development of cell polarity in yeast and beyond. Microbiol. Mol. Biol. Rev. *71*, 48–96.

Pashkova, N., Catlett, N. L., Novak, J. L., and Weisman, L. S. (2005). A point mutation in the cargo-binding domain of myosin V affects its interaction with multiple cargoes. Eukaryot. Cell *4*, 787–798.

Paterson, J. M., Ydenberg, C. A., and Rose, M. D. (2008). Dynamic localization of yeast Fus2p to an expanding ring at the cell fusion junction during mating. J. Cell Biol. *181*, 697–709.

Peter, B. J., Kent, H. M., Mills, I. G., Vallis, Y., Butler, P.J.G., Evans, P. R., and McMahon, H. T. (2004). BAR domains as sensors of membrane curvature: the amphiphysin BAR structure. Science *303*, 495–499.

Proszynski, T. J., Klemm, R., Bagnat, M., Gaus, K., and Simons, K. (2006). Plasma membrane polarization during mating in yeast cells. J. Cell Biol. *173*.

Pruyne, D., and Bretscher, A. (2000). Polarization of cell growth in yeast. I. Establishment and maintenance of polarity states. J. Cell Sci. *113*(Pt 3), 365–375.

Pruyne, D., Legesse-Miller, A., Gao, L., Dong, Y., and Bretscher, A. (2004). Mechanisms of polarized growth and organelle segregation in yeast. Annu. Rev. Cell and Dev. Biol. *20*, 559–591.

Pruyne, D. W., Schott, D. H., and Bretscher, A. (1998). Tropomyosin-containing actin cables direct the Myo2p-dependent polarized delivery of secretory vesicles in budding yeast. J. Cell Biol. *143*, 1931–1945.

Purcell, T. J., Morris, C., Spudich, J. A., and Sweeney, H. L. (2002). Role of the lever arm in the processive stepping of myosin V. Proc. Natl. Acad. Sci. USA *99*, 14159–14164.

Roberts, C. J., *et al.* (2000). Signaling and circuitry of multiple MAPK pathways revealed by a matrix of global gene expression profiles. Science *287*, 873–880.

Rose, M. D., Winston, F. M., Hieter, P., and Cold Spring Harbor Laboratory. (1990). Methods in Yeast Genetics: A Laboratory Course Manual, Cold Spring Harbor, NY: Cold Spring Harbor Laboratory Press.

Salminen, A., and Novick, P. J. (1987). A ras-like protein is required for a post-Golgi event in yeast secretion. Cell *49*, 527–538.

Schott, D., Ho, J., Pruyne, D., and Bretscher, A. (1999). The COOH-terminal domain of Myo2p, a yeast myosin V, has a direct role in secretory vesicle targeting. J. Cell Biol. *147*, 791–808.

Schott, D. H., Collins, R. N., and Bretscher, A. (2002). Secretory vesicle transport velocity in living cells depends on the myosin-V lever arm length. J. Cell Biol. *156*, 35–39.

Segall, J. E. (1993). Polarization of yeast cells in spatial gradients of alpha mating factor. Proc. Natl. Acad. Sci. USA *90*, 8332–8336.

Shaner, N. C., Campbell, R. E., Steinbach, P. A., Giepmans, B.N.G., Palmer, A. E., and Tsien, R. Y. (2004). Improved monomeric red, orange and yellow fluorescent proteins derived from *Discosoma* sp. red fluorescent protein. Nat. Biotech. *22*, 1567–1572.

Sivadon, P., Bauer, F., Aigle, M., and Crouzet, M. (1995). Actin cytoskeleton and budding pattern are altered in the yeast *rvs161* mutant: the Rvs161 protein shares common domains with the brain protein amphiphysin. Mol. Gen. Genet. *246*, 485–495.

Trueheart, J., Boeke, J. D., and Fink, G. R. (1987). Two genes required for cell fusion during yeast conjugation: evidence for a pheromone-induced surface protein. Mol. Cell. Biol. *7*, 2316–2328.

Uyeda, T. Q., Abramson, P. D., and Spudich, J. A. (1996). The neck region of the myosin motor domain acts as a lever arm to generate movement. Proc. Natl. Acad. Sci. USA *93*, 4459–4464.

Valdez-Taubas, J., and Pelham, H.R.B. (2003). Slow diffusion of proteins in the yeast plasma membrane allows polarity to be maintained by endocytic cycling. Curr. Biol. *13*, 1636–1640.

Walch-Solimena, C., Collins, R. N., and Novick, P. J. (1997). Sec2p mediates nucleotide exchange on Sec4p and is involved in polarized delivery of post-Golgi vesicles. J. Cell Biol. *137*, 1495–1509.

Wedlich-Soldner, R., Altschuler, S., Wu, L., and Li, R. (2003). Spontaneous cell polarization through actomyosin-based delivery of the Cdc42 GTPase. Science *299*, 1231–1235.

Whyte, J.R.C., and Munro, S. (2002). Vesicle tethering complexes in membrane traffic. J. Cell Sci. *115*, 2627–2637.

Wilkinson, L. E., and Pringle, J. R. (1974). Transient G1 arrest of *S. cerevisiae* cells of mating type alpha by a factor produced by cells of mating type a. Exp. Cell Res. *89*, 175–187.